

Formal analytical solutions for the Gross-Pitaevskii equation.

C. Trallero-Giner,^(a) Julio C. Drake-Perez,^(a) V. López-Richard^(b), and Joseph L. Birman^(c)

(a) Faculty of Physics, Havana University, 10400 Havana, Cuba

(b) Universidade Federal de São Carlos,

Departamento de Física, 13560-905, São Carlos, SP, Brazil.

(c) Department of Physics, The City College of CUNY, New York, NY 10031

(Dated: October 31, 2018)

Abstract

Considering the Gross-Pitaevskii integral equation we are able to formally obtain an analytical solution for the order parameter $\Phi(x)$ and for the chemical potential μ as a function of a unique dimensionless non-linear parameter Λ . We report solutions for different range of values for the repulsive and the attractive non-linear interactions in the condensate. Also, we study a bright soliton-like variational solution for the order parameter for positive and negative values of Λ . Introducing an accumulated error function we have performed a quantitative analysis with other well-established methods as: the perturbation theory, the Thomas-Fermi approximation, and the numerical solution. This study gives a very useful result establishing the universal range of the Λ -values where each solution can be easily implemented. In particular we showed that for $\Lambda < -9$, the bright soliton function reproduces the exact solution of GPE wave function.

PACS numbers: 03.75.Be, 03.75.Lm, 05.45.Yv, 05.45.-a

I. INTRODUCTION

Since the unambiguous experimental realization in dilute ultra-cold atom cloud of the Bose-Einstein condensed phase (BEC)^{1,2,3,4,5,6,7} a lot of work has been devoted for searching the dynamic and physical properties of the nonlinear matter waves and excitations of the condensate. The observation of this effect in dilute atomic gases has allowed to invoke the weakly interacting mean field theory to describe the properties of the BEC systems.^{8,9} Hence, the dynamics of the process for the order parameter has been ruled by equations of nonlinear Schrödinger (NLS) type and mainly by the Gross-Pitaevskii equation (GPE). Nowadays, NLS equations with attractive (negative scattering length)¹⁰ and repulsive (positive scattering length)¹¹ nonlinear interactions have been reported to describe experimental observations of different types of wave solitons.¹² Most of the theoretical work has been devoted to implement numerical solutions of the GPE for the order parameter (see Ref. [9] and references therein). To study and to control the physical properties of the condensate it will be very useful to manipulate analytical expressions for the chemical potential and for the order parameter as well. A typical example of the great physical interest is the attention devoted to the collective excitation spectrum of a BEC. In this case we have to deal with the time-dependent GP equation under the linear response approximation. Here, as input parameter, we have to insert in the Bogoliubov equations¹³ the order parameter and the chemical potential solution of the NLS. In that sense, some analytical results for those magnitudes are priceless. Also, many order problems can be stressed on the field of cold atoms BEC as the dynamical stability,¹⁴ atomic current in an optical lattice,¹⁵ etc.

In order to achieve closed solution the variational procedure with a Gaussian as a trial wave function has been proposed (see Ref. [16] and reference therein). Nevertheless, it is well known that this Ansatz does not reproduce well the properties of the condensate. For example, in the repulsive interaction case and in the strong nonlinear limit, the shape of the order parameter should be similar to the Thomas-Fermi (TF) solution (see below Eq. (4)). Moreover, the results obtained with the standard variational procedure is, in many cases, qualitative and, even if the real shape of the wave function resembles the trial wave function, the variational method is not always a good reference for solving nonlinear equations.¹⁷

Nowadays, available numerical methods for solving differential equations are fast and accurate. Nevertheless, if the evaluation of several physical magnitudes is carried out, such

as the optical properties among others, or to control the properties of the condensate (as we just discussed above), this advantage is lost due to cumbersome numerical computational procedures that must be performed at the end of the calculation. Moreover, if we work with a given basis of functions, it is difficult to know *a priori* if, in fact, the basis is a complete set for the Hilbert space of the specific nonlinear equation. Also, the type as well as the swiftness of convergence to the real solution is not always well established. In that sense, to implement manageable analytical expressions for the order parameter, where the accuracy and the absolute error of the obtained solution are controlled, has become a necessity. This is a fact in the study of nonlinear equation and in particular for the GPE.

A description of the order parameter $\Phi(x)$ in terms of a controlled truncated basis becomes a useful tool if we are dealing with not many implemented functions and the degree of accuracy is well established. So, the obtained expansion will be given by a sum of few basic functions, allowing in that way to handle with explicit solution to describe the physical properties of the condensate. Unfortunately, the beauty of such a mathematical result is restricted to certain range of values for the parameter involved in the nonlinear equation under study. The challenge is to find precisely this range of convergence, to give the absolute error in terms of physical parameters, and to provide other handled compact solutions outside the obtained range of the desire accuracy. We would like to remark that the most important requirements for analytical solutions are simplicity, flexibility, and the viability to be used in perturbation approaches for the calculations of physical properties.

In this paper we present different methods of solutions of the time independent GPE based on the equivalent integral GPE and its relation with the Green function of the corresponding linear operator, on the soliton solution, and on a bright soliton-like variational function. This discussion will provide general analytical expressions for the order parameter and for the chemical potential in a universal range of the non-linear interaction parameter.

To describe the order parameter $\Phi(x)$ we started with the isomorphic one-dimensional nonlinear Gross-Pitaevskii equation (GPE),^{8,9} which can be written as

$$-\frac{\hbar^2}{2m} \frac{d^2\Phi}{dx^2} + \frac{1}{2} m\omega^2 x^2 \Phi + \lambda |\Phi|^2 \Phi = \mu \Phi \quad (1)$$

with the normalization condition

$$1 = \int dx |\Phi|^2. \quad (2)$$

In the above equation μ represents the chemical potential, ω is the trap oscillator frequency, m is the alkaline atom mass, and λ is a self-interaction parameter describing the interaction between the particles.

Equation (1) presents an explicit solution if the non-linear term $\langle \lambda |\Phi|^2 \rangle$ is larger than the mean value of kinetic energy operator. This approximation, known as TF,^{18,19} provides simple expressions for the chemical potential and the wave function given by

$$\frac{\mu_{TF}}{\hbar\omega} = \left(\frac{3\sqrt{2}}{8}\Lambda\right)^{2/3}, \quad (3)$$

$$l_0 |\Phi_{TF}|^2 = \frac{1}{\Lambda} \left[\left(\frac{3\sqrt{2}}{8}\Lambda\right)^{2/3} - \frac{1}{2}\left(\frac{x}{l_0}\right)^2 \right], \quad (4)$$

where $\Lambda = \lambda/l_0\hbar\omega$, $l_0 = \sqrt{\hbar/m\omega}$, and the value of $\lambda \geq 0$ is restricted by Eq. (4).

The next section is devoted to develop the proposed methods to solve Eq. (1), beyond the above typical TF approximation, . The main goal is to obtain explicit representations for the whole range of the self-interaction parameter λ (negative and positive values) and to show the range of validity for each particular method of solution.

II. ANALYTICAL APPROACHES

First we will study the variational method based on a soliton wave function as Ansatz function, secondly we analyze the validity of the spectral method based on the equivalency between the integral and differential equation (1) and the Green function, solution of the linear harmonic oscillator operator. Moreover, using the obtained general formalism we report perturbation solutions for Φ and μ in terms of the non-linear parameter λ . For sake of comparison and in order to check the accuracy of the implemented approaches, the numerical solution of Eq. (1) is also addressed.

A. Variational method: Soliton approach

The variational method, valid for positive as well as negative values of λ , could provide a simple picture of the main physical characteristics of the BEC. Without the trap potential,

the GPE (1) reduces to the nonlinear Schrödinger equation which for $\lambda < 0$ admits the stationary normalized *bright soliton* solution

$$\Phi_S(x, K) = \left(\frac{K}{2}\right)^{1/2} \text{sech}(Kx). \quad (5)$$

Here, the chemical potential μ_S and the inverse of the soliton length K are expressed by

$$\mu_S = -\frac{m\lambda^2}{8\hbar^2}, \quad K = \frac{m\lambda}{2\hbar^2}. \quad (6)$$

In order to solve Eq. (1) for all values of λ we propose as variational Ansatz the bright soliton (5) where K is taken as a variational parameter. The Ritz's variational method applied to the NLS (1) provides for the chemical potential $\mu(K)$ the parametric equation (see Appendix A)

$$\mu_{var}(K) = \frac{\hbar^2 K^2}{2m} \alpha + \frac{m\omega^2}{2K^2} \beta + \frac{K\lambda}{4} \gamma, \quad (7)$$

where K must fulfill the dimensionless equation

$$b^4 + b^3 - \delta = 0 \quad (8)$$

with $b = K\hbar^2/(m\lambda)$ and $\delta = (1/\Lambda)^4 \pi^2/4$. Accordingly, Eq. (7) is reduced to the simple relation

$$\frac{\mu_{var}}{\hbar\omega} = -\frac{1}{6} \Lambda^2 \left(b^2 - \frac{3\delta}{b^2}\right) \quad (9)$$

and for the order parameter we get

$$\sqrt{l_0} \Phi_{var} = \left(\frac{\Lambda b}{2}\right)^{1/2} \text{sech}\left(\Lambda b \frac{x}{l_0}\right). \quad (10)$$

Equation (8) is a fourth-degree algebraic equation with only one real physical meaningful solution, which depends on the sign of the non-linear interaction parameter Λ . In order to get a more clear view of the solution for Eq. (8), we carry out separate calculations at $\Lambda = 0$ and for the strong repulsive (attractive) limit $\Lambda \rightarrow \infty$ ($\Lambda \rightarrow -\infty$).

If $\Lambda \rightarrow 0$ we obtain from Eqs. (8) and (9)

$$b \times \Lambda = \sqrt{\frac{\pi}{2}} \quad (11)$$

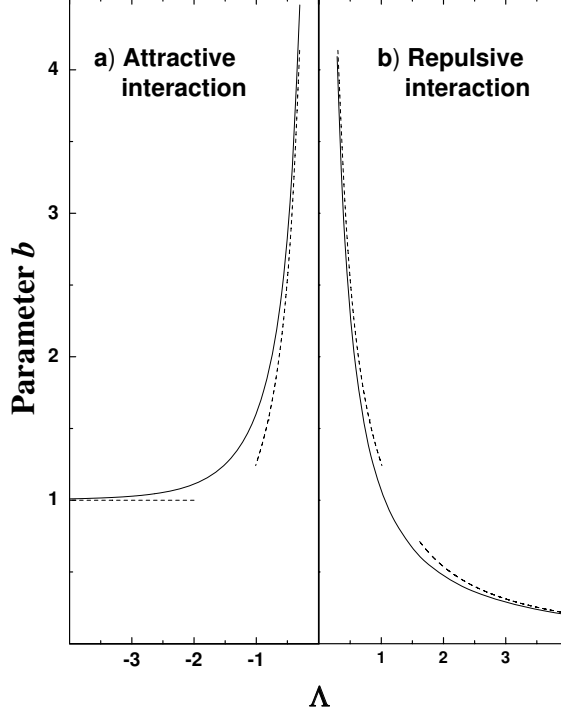


FIG. 1: Variational parameter b as a function of Λ . The asymptotic limits (13) and (15), and the behavior at $\Lambda \approx 0$, Eq. (11), are indicated by dashed lines.

and

$$\frac{\mu_{var}(\Lambda = 0)}{\hbar\omega} = \frac{\pi}{6}. \quad (12)$$

In the strong attractive limit ($\Lambda \ll -1$) and keeping the leading term in Eq. (8), the possible physical solution has the asymptotic behavior

$$b(\Lambda \rightarrow -\infty) = 1 + o\left(\sqrt{\frac{\pi}{2}} \frac{1}{\Lambda}\right)^{\frac{7}{3}} \quad (13)$$

and the chemical potential μ is given by

$$\frac{\mu_{var}(\Lambda \rightarrow -\infty)}{\hbar\omega} = -\frac{1}{6}\Lambda^2. \quad (14)$$

In the repulsive limit case, $\Lambda \gg 1$, Eq. (8) yields

$$b(\Lambda \rightarrow \infty) = o\left(\sqrt{\frac{\pi}{2}} \frac{1}{\Lambda}\right)^{\frac{4}{3}} + o\left(\sqrt{\frac{\pi}{2}} \frac{1}{\Lambda}\right)^{\frac{7}{3}} \quad (15)$$

with

$$\frac{\mu_{var}(\Lambda \rightarrow \infty)}{\hbar\omega} = \left(\frac{\pi\sqrt{2}}{8}\right)^{\frac{2}{3}} (\Lambda)^{\frac{2}{3}}. \quad (16)$$

We can compare the above limit solutions with those obtained by the TF approximation, Eq. (3), and the exact soliton solution, Eq. (6). The relative errors are equal to

$$\left| \frac{\mu_{var}(\infty) - \mu_{TF}(\infty)}{\mu_{TF}(\infty)} \right| = \left(\frac{\pi}{3} \right)^{\frac{2}{3}} - 1 \approx 0.0312. \quad (17)$$

and

$$\left| \frac{\mu_{var}(-\infty) - \mu_S(\infty)}{\mu_S(\infty)} \right| = \left| -\frac{8}{6} + 1 \right| \approx 0.3333. \quad (18)$$

From the above relations we conclude that the variational wave function (5) provides a better solution of the GPE in the strong repulsive case than for the attractive one. At $\Lambda = 0$ a relative error of 0.0472 is reached by comparing Eq. (12) with the exact solution of the harmonic oscillator problem $\mu/\hbar\omega = 0.5$. In Fig. 1 we present the parameter b , solution of the Eq. (8), as a function of the dimensionless parameter Λ . Also, the limit solutions are indicated by dashed lines. It can be seen that the calculated asymptotic behaviors (11), (13), and (15) at $\Lambda = 0$, $\Lambda \rightarrow -\infty$, and $\Lambda \rightarrow \infty$, respectively, are quickly reached by the exact solutions of Eq. (8). It is not surprising that the Ritz's variational method failed to get a closed analytical solution of the differential GPE. The variational method here implemented is only valid for linear differential equations or the corresponding Lagrangian of the problem.

B. GP integral equation: Green function solution

One of the most powerful analytical method used to solve differential and integral equations corresponds to the Green function formalism (GFF). In order to implement this mathematical technique to the non-linear Schrödinger equation we rewrite (1) as

$$L_0[\Phi] = -\frac{\hbar^2}{2m} \frac{d^2\Phi}{dx^2} + \frac{1}{2}m\omega^2 x^2\Phi = f(x). \quad (19)$$

Here $f(x)$ will be considered as an inhomogeneity in the differential equation and equal to

$$f(x) = (\mu - \lambda |\Phi(x)|^2)\Phi(x).$$

Function $\Phi(x)$, solution of Eq. (19), can be cast in terms of the Green function $G(x, x')$ of the linear operator $L_0[\Phi]$. Formally, we can write $\Phi(x)$ as a function of the inhomogeneity $f(x)$ as²⁰

$$\Phi(x) = \int_{-\infty}^{\infty} G(x, x')(\mu - \lambda |\Phi(x')|^2)\Phi(x')dx'. \quad (20)$$

The above expression corresponds to the GP integral equation for the order parameter $\Phi(x)$. We observe that the integral equation (20) has a symmetric kernel, $G(x, x')$, which fulfills the differential equation

$$L_0 [G(x, x')] = \delta(x - x').$$

To write the formal solution (20) in terms of the Green function of the operator L_0 , the function $f(x)$ has some constraints.^{21,22} In our case, all functions and the Green function also, have to fulfill the boundary condition $\Phi(x) \rightarrow 0$ as $x \rightarrow \pm\infty$. This guarantees that the inhomogeneity $f(x)$ belongs to the same Hilbert space of the linear operator L_0 . The kernel $G(x, x')$ is the given by the following spectral representation

$$G(x, x') = \sum_{n=0}^{\infty} \frac{\varphi_n(x)\varphi_n(x')}{\hbar\omega(n + 1/2)}, \quad (21)$$

with $\varphi_n(x)$ being the harmonic oscillator wave function²³

$$\varphi_n(x) = \left(\frac{1}{\pi^{1/2} 2^n n! l_0} \right)^{1/2} \exp\left(\frac{-x^2}{2l_0^2} \right) H_n\left(\frac{x}{l_0} \right). \quad (22)$$

We have to note that according to the general theory of Fredholm integral equations,^{21,22} the set of functions appearing in the spectral representation of a symmetric kernel, $\{\varphi_n(x)\}$ in the present case, represents a complete set of functions for the given Hilbert space of the GP integral equation (20). Hence, the convergence of the expansion (21) is guaranteed and we can insert the spectral representation of $G(x, x')$ in (20) and interchange the integral and infinity expansion (21). Thus

$$\Phi = \sum_{n=0}^{\infty} \frac{\varphi_n(x)}{\hbar\omega(n + 1/2)} \int \varphi_n(x')(\mu - \lambda |\Phi(x')|^2)\Phi(x')dx'. \quad (23)$$

From (23) it is straightforward that the general solution for the order parameter Φ has an explicit representation through the harmonic oscillator $\varphi_n(x)$ as

$$\sum_{n=0}^{\infty} \varphi_n(x)C_n(\mu). \quad (24)$$

Since the inhomogeneity $f(x)$ belongs to the same Hilbert space of the symmetric kernel of the Fredholm integral equation (20), the convergency of the series (24) in energy to the function Φ is guaranteed.²⁴

In the present case the coefficients $C_n(\mu)$ are restricted to obey the relation

$$C_n = \int \frac{1}{\hbar\omega(n+1/2)} \varphi_n(x') (\mu - \lambda |\Phi(x')|^2) \Phi(x') dx'. \quad (25)$$

Inserting the convergent series (24) in Eq. (25), it follows that the vector coefficient $\mathbf{C}(\mu)$ must fulfil the non-linear equation system

$$[\mathbf{\Delta}(\mu) + \Lambda \bar{\mathbf{C}} \cdot \mathbf{T} \cdot \mathbf{C}] \mathbf{C} = 0, \quad (26)$$

where

$$\Delta_{nm} = \left(n + \frac{1}{2} - \frac{\mu}{\hbar\omega} \right) \delta_{nm}. \quad (27)$$

and T_{plmn} is a fourth dimensional matrix defined in the Appendix B.

The order parameter Φ and the chemical potential as a function of the dimensionless parameter Λ are obtained by solving the non-linear equation system (26). Although the mathematical complexity of Eq. (1) has been reduced, Eq. (26) is nevertheless an infinite generalized eigenvalue problem for $\mu(\Lambda)$ and $\mathbf{C}(\mu(\Lambda))$. The complexity of the problem depends on the sign and the values of the non-linear parameter λ but the key issue is how quickly converges the series in (24) or equivalently, the non-linear equation system (26). This important problem is addressed in the next section.

We have to mention that the obtained problem (26) is isomorphic to Galerkin method. The former one is a generalized variational method where for a given equation $L[F] = L_0[F] + L_p[F]$ it is possible to choose a certain basis $\{g_k\}$ of the operator L_0 and to expand the function F in term of the given basis. The choice of the operator L_0 (which must include the boundary conditions) is not unique and certain degree of freedom prevails. To guarantee that the expansion converge to the real solution, the picked out operators L_0 and L_p have to fulfil certain mathematical conditions (see Ref. [24] for a detailed description of this mathematical treatment). This crucial question is not trivial when we are dealing with non-linear equations as the NLS. In our case the mathematical treatment above developed is based on the properties of the Fredholm integral equations and can be considered a rigorous demonstration of the validity of the expansion (24) and the convergence to the correct solution.

We obtained the ground state solution Φ_0 in terms of a truncated basis set, $\{\varphi_n(x)\}$ ($n = 1, \dots, I$), by defining the finite dimensional nonlinear Hill determinant eigenvalue equation²⁵

$$\|\mathcal{M}^{(I)}(\mu(\Lambda), \mathbf{C})\| = 0, \quad (28)$$

where $\mathcal{M}_{nm}^{(I)}$, ($n, m = 1, 2, \dots, I$) are the corresponding matrix elements according to the Eq. (26). Since the scaling of any direct numerical algorithm of integration implemented to obtain the tensor T_{plmn} is of the order $I^4 \times P$ (P is the number of grid points) the numerical implementation becomes a cumbersome task and non-efficient method of evaluation. To get a better efficient algorithm than those based on a direct numerical integration of the tensor T_{plmn} , it is necessary to exploit its analytical representation together with its symmetry properties. This analysis is presented in the Appendix B allowing a straightforward evaluation of the tensor T_{plmn} .

To solve Eq. (28), we have implemented the Neumann iterative procedure in a finite basis of dimension I . For a given iteration and since the functions $\{\varphi_n(x)\}$ define a complete set for the GPE, obeying the natural boundary conditions, $\varphi_n(x) \rightarrow 0$ for $x \rightarrow \pm\infty$, the roots of the determinant (28) converge to the exact ground state solution of Eq. (20) and $\lim_{I \rightarrow \infty} \mu^{(I)}(\Lambda) = \mu(\Lambda)$.²⁵ The numerical procedure starts from a trial vector $\mathbf{C} \sim \tilde{\mathbf{C}}$ and iteratively we obtain the k -th approximation. In each step, the matrix (28) must be recalculated by using the new eigenvector $\mathbf{C} \sim \tilde{\mathbf{C}}$. The procedure is repeated until $|C_n^{(k)} - C_n^{(k-1)}| < \delta_c$ and (or alternatively) $|\mu^{(k)} - \mu^{(k-1)}| < \hbar\omega \cdot \delta_\mu$, where δ_c and δ_μ are the desirable accuracies for the coefficients and the chemical potential, respectively. For the iterative procedure, it is useful to introduce a control parameter $\varepsilon \in [0, 1]$, so that

$$\tilde{C}_n = \sqrt{\varepsilon(C_n^{(k-1)})^2 + (1 - \varepsilon)(C_n^{(k)})^2}.$$

This procedure is faster and accurate for positive and small negative values of the non-linear parameter $\Lambda > -5$. For $\Lambda < -5$ however, the size of the matrix we have to deal with grows as $|\Lambda|$ does. In the former case, a basis set of 25 functions allows at least 5 significant figures in the calculation of μ , while for the later at least 50 oscillator wave functions $\{\varphi_n\}$ were sorted in order to reach the same accuracy at $\Lambda = -10$.

According to the Neumann iterative procedure we have to introduce an initial starting $\mathbf{C}^{(0)}$ vector. This vector can be chosen according to the desirable Λ value and the following

criteria can be established: i) For the dimensionless interaction parameters $|\Lambda| < 1.5$, the coefficients $C_{n,m}^{(0)} = \delta_{n,m}$. ii) If $\Lambda > 5$ the asymptotic limit of the TF approximation wave function given by (4) is a good starting iterative procedure. iii) For attractive interaction and $\Lambda < -1.5$ the soliton wave function approach (5) is useful as initial condition .

C. Perturbation theory

It is useful to get expressions for μ and the order parameter Φ through a perturbation approach since these are easily handled solutions. Also, the explicit perturbation expressions can be implemented as a method to control other solutions in particular the numerical ones. If the nonlinear term $H_p = \lambda |\Phi|^2$ is considered as a perturbation in comparison to the trap potential $m\omega^2 x^2/2$, the chemical potential and the vector \mathbf{C} in Eq. (26) can be sought in the form of series, i.e.

$$\begin{aligned} C_m &= C_m^{(0)} + \lambda C_m^{(1)} + \lambda^2 C_m^{(2)} + \dots, \\ \mu &= \mu^{(0)} + \lambda \mu^{(1)} + \lambda^2 \mu^{(2)} + \dots \end{aligned}$$

Taking only the second order interaction in λ , Eq. (26) yields

$$\mu = \frac{\hbar\omega}{2} + \frac{\lambda}{l_0} T_{0000} - 3 \left(\frac{\lambda}{l_0} \right)^2 \sum_{m=1}^{\infty} \frac{|T_{000m}|^2}{\hbar\omega m}. \quad (29)$$

Using the properties of the matrix T_{plmn} given in the Appendix B we get

$$\frac{\mu}{\hbar\omega} = \frac{1}{2} + \frac{\Lambda}{\sqrt{2\pi}} - \frac{3}{2\pi} \Lambda^2 \sum_{m=1}^{\infty} \frac{(2m-1)!}{2^{4m} (m!)^2}. \quad (30)$$

Using that

$$\sum_{m=1}^{\infty} \frac{(2m)!}{2^{3m} (m!)^2 m (x^2 + 1)^m} = -2 \ln \left(\frac{1}{2} \sqrt{\frac{2x^2 + 1}{2(x^2 + 1)}} + \frac{1}{2} \right)$$

the chemical potential up to second order is reduced to the following useful expression

$$\frac{\mu}{\hbar\omega} = \frac{1}{2} + \frac{\Lambda}{\sqrt{2\pi}} - 0.033106 \times \Lambda^2. \quad (31)$$

Finally, the normalized order parameter Φ including terms to the first order can be expressed as

$$\Phi = \varphi_0(x) + \frac{\Lambda}{\sqrt{2\pi}} \sum_{m=1}^{\infty} \frac{(-1)^{m+1} \sqrt{(2m)!}}{2^{2m} (m!) 2m} \varphi_{2m}(x). \quad (32)$$

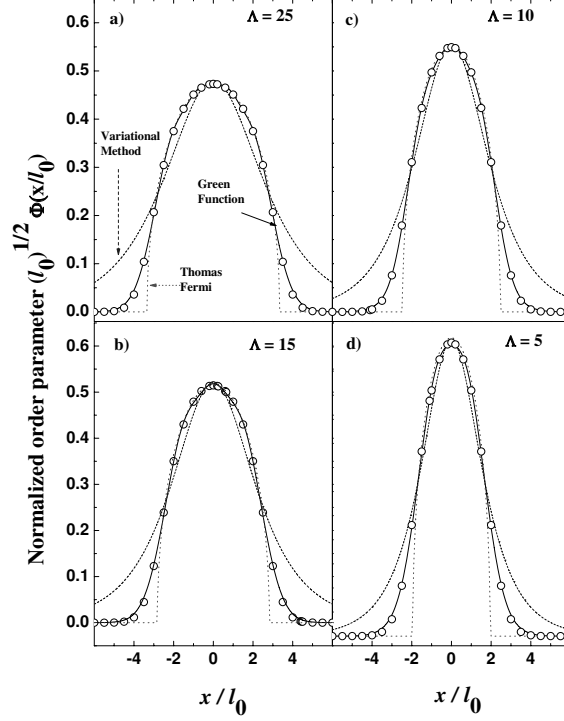


FIG. 2: (Color online) Normalized order parameter $\sqrt{l_0}\Phi(x/l_0)$ for the positive dimensionless self-interaction Λ values: a) 25, b) 15, c) 10, and d) 5. Solid line: Solution (24). Dashed line: Soliton variational approach. Dot: Thomas-Fermi approximation. Empty circles: Numerical solution.

D. Numerical Solution

A comparison of the obtained analytical solutions with direct numerical calculations is an important control for validating the mathematical methods here introduced. In order to solve (1) numerically, we choose a finite difference method where for the second derivative we select a simple three-points approximation with uniform spacing, so that the differential equation can be rewritten as a symmetrical tri-diagonal matrix. The eigenvalue problem for the obtained matrix can then be solved by the usual methods. Explicitly we have

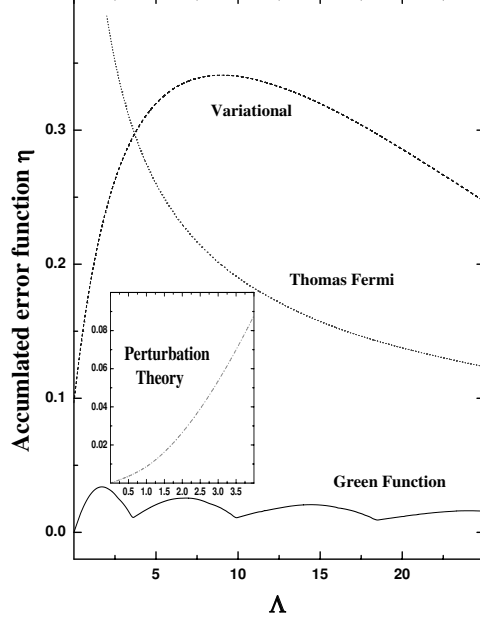


FIG. 3: (Color online) Accumulated error function η for the repulsive interaction as a function of Λ . Solution (24) (solid line), soliton variational approach (10) (dashed line), and Thomas-Fermi function (4) (dot line). Inset: Perturbation wave function (32) (dot-dashed line).

$$\begin{aligned}
 & \begin{pmatrix} v_1 & -\delta^{-2} & & & & \\ -\delta^{-2} & v_2 & & & & \\ & & \ddots & & & \\ & & & \ddots & & \\ & & & & v_{L-1} & -\delta^{-2} \\ & & & & -\delta^{-2} & v_L \end{pmatrix} \begin{pmatrix} \overline{\Phi}_1 \\ \overline{\Phi}_2 \\ \cdot \\ \cdot \\ \overline{\Phi}_{L-1} \\ \overline{\Phi}_L \end{pmatrix} \\
 &= \frac{\mu}{\hbar\omega} \begin{pmatrix} \overline{\Phi}_1 \\ \overline{\Phi}_2 \\ \cdot \\ \cdot \\ \overline{\Phi}_{L-1} \\ \overline{\Phi}_L \end{pmatrix}, \tag{33}
 \end{aligned}$$

where

$$v_i = v_i(\overline{\Phi}_i) = \frac{1}{2} \left(-\frac{L}{2l_0} + (i-1)\delta \right)^2 + \Lambda |\overline{\Phi}_i|^2 \delta^{-1} + \delta^{-2}, \quad (34)$$

$\overline{\Phi}_i = \sqrt{l_0}\Phi_i$, $\overline{\Phi}_i = \overline{\Phi}(-\frac{L}{2l_0} + (i-1)\delta)$, $i = 1, 2, \dots, L$, and δ is the discrete step. The presence of the wave function inside the matrix in the left side of Eq. (33) enforces the use of some kind of iteration procedure in order to solve the non-linear problem. That is, for the vector \mathbf{v} of components v_i (see Eq. (34)) we set

$$\mathbf{v} [\mathbf{F}^{(k)}], \quad k = 0, 1, 2, \dots, \quad (35)$$

where $\mathbf{F}^{(k)}$ is a certain trial function. We started with certain $F^{(0)}(x) = \overline{\Phi^{(0)}(x)}$ evaluated at the x_i mesh points. After that, we find the approximate eigenvector Φ and eigenvalue μ of the ground state solution of Eq. (33). The new trial function $\mathbf{F}^{(k)}$ is obtained by the expression

$$F_i^{(k)} = \sqrt{\varepsilon \left[\overline{\Phi_i^{(k-1)}} \right]^2 + (1 - \varepsilon) \left[\overline{\Phi_i^{(k)}} \right]^2}$$

with $\varepsilon \in [0, 1]$. This procedure is repeated until $\left| \overline{\Phi_i^{(k)}} - \overline{\Phi_i^{(k-1)}} \right| < \delta_\Phi$ and (or alternatively) $|\mu^{(k)} - \mu^{(k-1)}| < \hbar\omega \cdot \delta_\mu$, where δ_Φ and δ_μ are the desirable accuracies for the wave function and the chemical potential, respectively. A similar procedure has been used with success in Ref. [26] for a two component BEC. The practical implementation of the above described method is mainly straightforward, however, due to the influence of the non-linear term, the accuracy and speed of convergence is critically dependent on the correct choice of the parameter ε . Our experience shows that the best value ε depends on the value and sign of the non-linear term.

III. RESULTS

We shall now discuss the accuracy and the reliability of the above implemented methods of solution, by studying independently the repulsive and the attractive interaction cases.

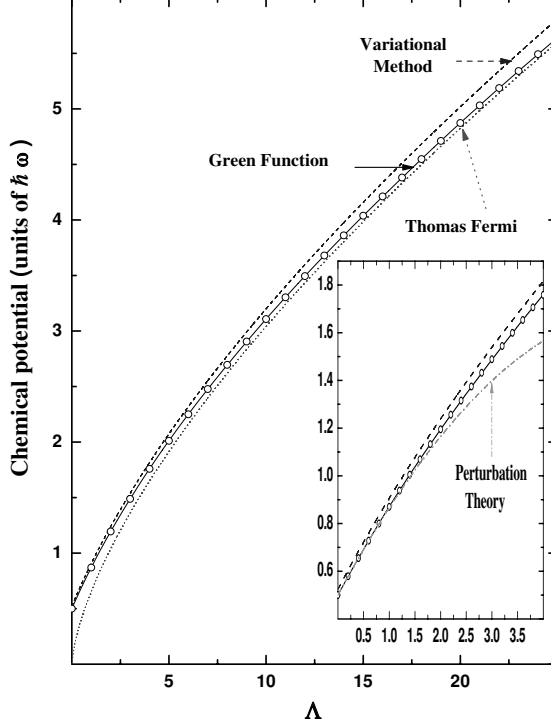


FIG. 4: (Color online) Chemical potential in units of $\hbar\omega$ as a function of dimensionless self-interaction parameter Λ . Solid line: Equation (26). Dashed line: Soliton variational approach (9). Dotted line: Thomas-Fermi approximation (3). Empty dot: Numerical solution. Inset: Perturbation theory (31) (dot-dashed line).

A. Repulsive interaction

Figure 2 displays the order parameter $\sqrt{l_0}\Phi(x/l_0)$ for several values of Λ . The variational solution of the Eqs. (9) and (10) is represented by dashed lines, solid lines present the calculation using Eq. (24), and the TF approach, following Eq. (4), is indicated by dots. Empty circles show the obtained numerical solutions of the GPE (1) following the procedure described in Sec. II D. It can be seen that the wave function is more delocalized and the maximum of $\Phi(x/l_0)$ decreases as Λ increases, thus the condensate spreads as the non-linear term increases. Also, in Fig. 2, the differences between all calculated analytical representations and the numerical procedure are qualitatively displayed. As already known, the TF approach reproduces well the properties of the condensate for large values of Λ , while the proposed variational solution exhibits a better approximation for small values of Λ . In general, we have obtained very good agreement between the solution (24) and the numerical

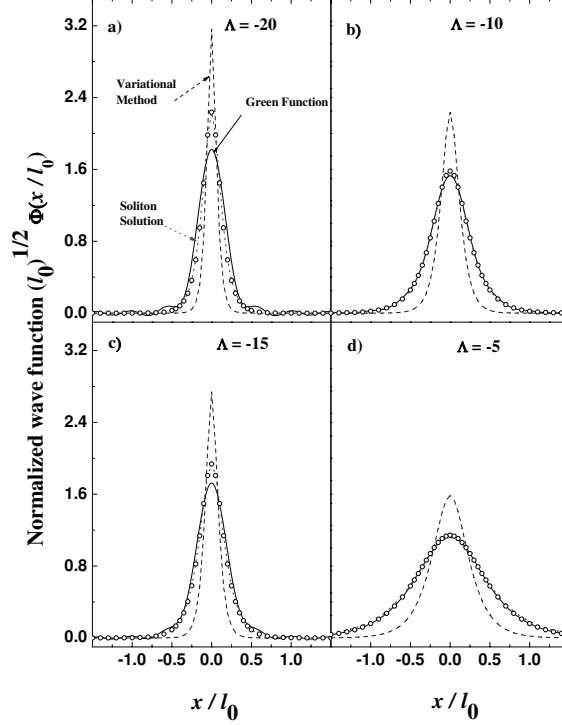


FIG. 5: (Color online) The same as Fig. 2 for the attractive dimensionless self-interaction Λ values: a) -20, b) -15, c) -10, and d) -5. Dotted line represents the soliton solution (5).

solution for all considered values of dimensionless interaction parameter Λ . Nevertheless, it is useful to define a magnitude that quantify the quality of the implemented analytical solutions. Hence, we have introduced the accumulated error function

$$\eta_i = \int_{-\infty}^{\infty} |\Phi_{num}(x) - \Phi_i(x)| dx, \quad (36)$$

where Φ_{num} is the numerical solution of Eq. (1). The above magnitude gives a direct estimation of the total error introduced throughout the whole interval $-\infty < x < \infty$. Since in each given point $x \in (-\infty, \infty)$ we add the modulus of the difference between $\Phi_{num}(x)$ and $\Phi_i(x)$, then η_i determines the maximum accumulated error for the analytical wave function $\Phi_i(x)$. Figure 3 presents the estimated error η_i as a function of the dimensionless interaction term Λ for all functions considered: the Thomas-Fermi (dot line), the solution (24) (solid line), and the soliton variational approach (dash line). From the figure it can be seen that the best analytical solution ($\eta < 0.033$) is reached by using (24), while the TF approximation approaches, asymptotically, to the exact solution. The soliton variational solution exhibits its minimum error ($\eta < 0.2$) for $\Lambda < 2$, reaching a maximum error at $\Lambda \approx 10$. One can notice

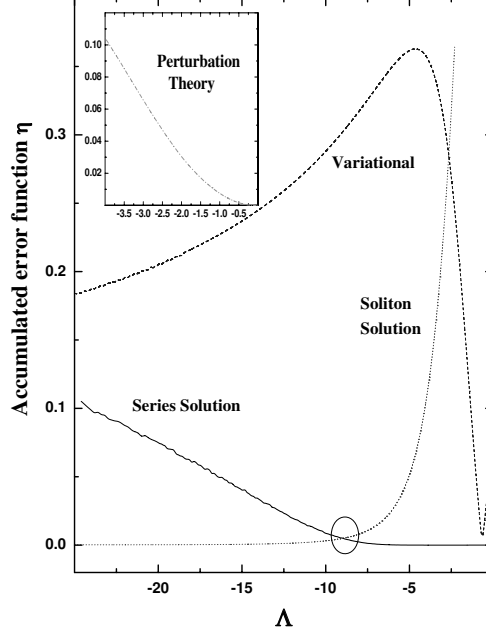


FIG. 6: (Color online) The same as Fig. 3 for the attractive interaction as a function of Λ . Dotted line represents the soliton solution (5). Inset: Accumulated error function η for the perturbation wave function (32) (dot-dashed line).

that Φ_{var} is a better approach than the TF for $\Lambda < 3.6$. The accumulative error introduced by the perturbation wave function (dash-dot line) is also shown in the inset. In general, the accuracy of the series (24) can be greatly improved if large matrixes are implemented. In our calculations a few functions (a 50×50 matrix) was necessary to achieve an accuracy of 10^{-8} for the chemical potential. In the case of the numerical procedure (33), values of $\mu/\hbar\omega$ were calculated with an uncertainty of 10^{-10} .

In Fig. 4, we compare the calculated chemical potential in units of the energy trap $\hbar\omega$ according to the analytical methods outlined in the previous section. The Thomas-Fermi approach following Eq. (3) is indicated by dots, the soliton variational solution obtained by solving the Eqs. (8) and (9) is represented by a dashed line, while the solid line presents the calculation using the Hill determinant (28). In the inset, the comparison with the perturbation theory given by Eq. (31) (dash dot line) is also shown. The numerical solution is also presented by empty dots. As expected the TF limit increases its accuracy, i.e., less than 3% of error at $\Lambda = 10$, as the non-linear parameter increases. No differences can be observed in the scale of the figure between the numerical solution and the chemical potential

using Eq. (28). The soliton variational calculation presents a larger error for $\Lambda > 7$. Also, in the figure we can observe the relative error of 0.0312 between the TF and variational solutions as reported by the Eq. (17) at $\Lambda \rightarrow \infty$. Concerning the perturbation theory, the best accuracy, less than 3%, is reached for $\Lambda < 2$. The results shown in the Figs. 3 and 4 have a universal character and the comparison between the analytical methods provides universal criteria of their validity ranges.

B. Attractive interaction

Following the same trends as in the repulsive case, Fig. 5 shows the normalized order parameter for four negative values of Λ . In the figure, the dotted line represents the soliton solution (5). We observe that using the series (24) the agreement is not so wide ranging as for the repulsive case. For values of $\Lambda > -10$, we obtain a better match between the Eq. (24) and the numerical solution (33). Nevertheless, the agreement reached with the soliton solution (5) is remarkably good. In order to quantify the discrepancy between the

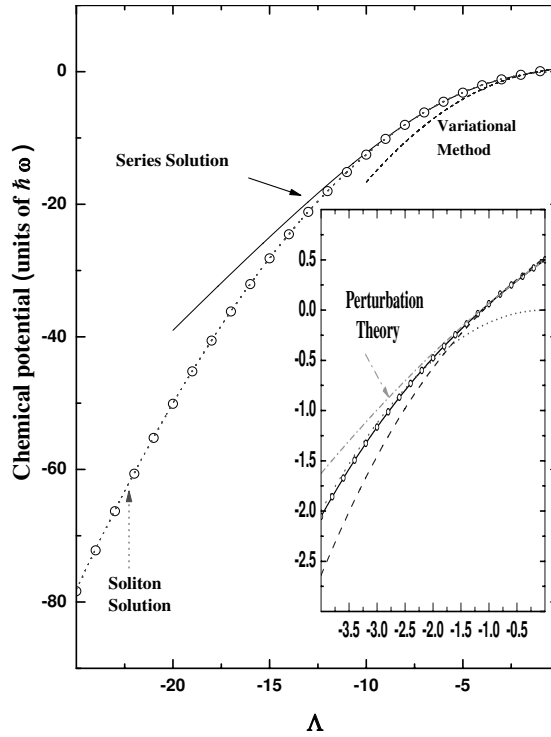


FIG. 7: (Color online) The same as Fig. 4 for the attractive interaction as a function of Λ . Dotted line represents the soliton chemical potential (6). Inset: Perturbation theory (31) (dot-dashed line)

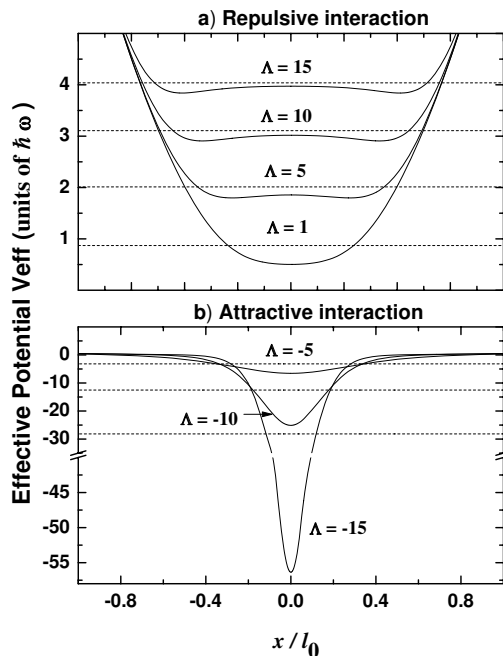


FIG. 8: Effective Potential V_{eff} for the GPE (see text).

implemented analytical solutions and the numerical one, we evaluate the accumulated error (36) in terms of Λ . Figure 6 presents η_i for all considered functions Φ_i . Here, a dotted line is used for the soliton solution (5). We have estimated that the best result by using Eq. (24) is reached, for $\Lambda \gtrsim -10$, while the exact soliton solution gives a better approach for $\Lambda < -10$, and in both cases we have an accumulated error $\eta < 0.005$. The soliton variational solution Φ_{var} yields a maximum error of $\eta \approx 0.36$ at $\Lambda \approx -4.6$. The accumulated error using the perturbation wave function (dash-dot line) is also shown in the inset and as expected $\eta \rightarrow 0$ as $\Lambda \rightarrow 0$.

Figure 7 depicts the calculated chemical potential μ for the variational calculation (Eqs. (8) and (9)), the solution following Eq. (28), soliton solution (6), and the numerical implementation for the GPE. The numerical procedure for the calculation of $\mu/\hbar\omega$ was implemented in order to achieve a maximum uncertainty of 10^{-10} . According to the results of Fig. 7, the system (26) using 50×50 matrix reproduces quite well the chemical potential values in the interval $\Lambda > -10$ with an accuracy less than 1.2%, while for μ_s , given by (6), the relative error tends to zero as Λ decreases. The best accuracy for the solution (9) is reached in the interval $-3 < \Lambda < 0$ and fails for smaller values of Λ . In the inset, we show the calculated

chemical potential in the framework of a perturbation method, Eq. (30), and compared with the other four methods. Here, it can be seen the strong deviation of the soliton solution from the correct values for $\Lambda > -2$. However, no differences are observed between the numerical, perturbation method, and the calculations using (26). Again as in the repulsive case, the results shown in Figs. 6 and 7 are of universal validity, giving an absolute estimation of the accuracy of each employed method as a function of a unique dimensionless parameter Λ . The present results teach us the way to get simple and exact analytical solutions for the GPE in the attractive interaction case in terms of Λ . Indeed, for $\Lambda \gtrsim -10$ using a small base (of the order of 50 oscillator wave functions) we obtain an accuracy of 10^{-8} for the chemical potential along with a minimum accumulated error, η , of 0.005 for the order parameter. For smaller values of Λ the soliton solution (5) and (6) can be implemented as the exact solution of Eq. (1). At this point, it is necessary to analyze the convergence to the exact solution provided by the series (24). In principle, as it was derived in Sec. II, the function (24) is an exact representation of the order parameter Φ with a convergence at list in energy to the real order parameter Φ . The basis $\{\varphi_n(x)\}$ is a complete set for the Hilbert space defined by Eq. (1) independent of the sign of the non-linear interaction term. Nevertheless, the number of the harmonic oscillator wave functions needed to reach the necessary convergence to the real solution depends on the values and sign of Λ . The key point is to know when the series (24) is really a good method for calculations and more efficient than the numerical ones. In our case, we selected 50 even functions φ_n reaching an accuracy for the chemical potential less than 10^{-8} in the range $-10 < \Lambda < 25$. To get the same accuracy for the chemical potential in the attractive region with $\Lambda < -10$, it is necessary to deal with matrixes (28) of rank larger than 50×50 .

In order to clarify this peculiarity of the expansion (24) we define the effective potential

$$Veff = \frac{1}{2}m\omega^2x^2 + \lambda|\Phi_{num}|^2,$$

where the order parameter Φ has been substituted by the numerical solution Φ_{num} . Figure 8 shows the potential $Veff$ in units of $\hbar\omega$ for both, the attractive and repulsive interactions. In the figure, we represented the exact calculation of μ for each considered value of Λ . It becomes clear that for the repulsive case, $Veff$ resembles the harmonic oscillator potential (Fig. 8 a)) and the chemical potential falls within certain range of the harmonic oscillator eigenvalues. Hence, the complete set of harmonic wave function $\{\varphi_n(x)\}$ can reproduce well,

with an inexpensive computational effort, the mathematical properties of the GPE. In the case of attractive interaction, see Fig. 8 b), the situation changes drastically. Here, the effective potential becomes more localized as Λ decreases and for $\Lambda \rightarrow -\infty$, $V_{eff} \sim \delta(x)$. The function V_{eff} does not resemble the harmonic oscillator potential, thus the values of the chemical potential are far away from $(n + \frac{1}{2})$ eigenvalues. Although the basis $\{\varphi_n(x)\}$ is complete, the number of functions $\varphi_n(x)$ needed to describe the order parameter Φ and chemical potential μ with certain accuracy should increase enormously as Λ decreases. This performance of the attractive interaction, determines that the Green function solution or equivalently the Galerkin or spectral method becomes computational expensive and the method is not adequate to describe the GPE for strong attractive interaction case, that is for $\Lambda < -10$.

IV. CONCLUSIONS

We have provided simple analytical forms to get explicit solutions for the GPE. The reported analytical techniques allow us to explore regions of positive and negative nonlinear interactions in condensates. We estimated the range of applicability of the perturbation theory, Thomas-Fermi approximation, soliton wave function, soliton variational calculation, and Green function solution (spectral method) through a universal interaction parameter $\Lambda = \lambda/l_0\hbar\omega$. The perturbation method is valid in the weak interaction limit, $-2 l_0\hbar\omega < \lambda < 2 l_0\hbar\omega$ with an error for the chemical potential less than 1.5% while the TF approximation provides an error less than 3% if $\lambda \gtrsim 10 l_0\hbar\omega$. The solution (24) with solely 50 harmonic oscillator wave functions reproduces quite well the chemical potential μ with an accuracy of 1.2% in the interval $-10 l_0\hbar\omega < \lambda < 10 l_0\hbar\omega$. We identified that the series (24) or the spectral method is not adequate and can be computational expensive for the attractive case if $\lambda < -10 l_0\hbar\omega$ (see Figs. 6, 7 and 8). In this case, the bright soliton solutions (5) and (6) represent the better approach for the order parameter and the chemical potential respectively. The presented soliton limit is formally equivalent to the Thomas-Fermi one and becomes a powerful tool for condensates with strong attractive interaction. Also, we have introduced a soliton variational procedure valid for repulsive and attractive interactions which can be applied to the study of the dynamics of BEC or to model physical systems obeying the GPE. With the present results it is possible to have a short and comprehensive discussion on the

usefulness of different approaches for the mathematical and physical description of the BEC.

We should note that the mathematical models here developed can be straightforward extended to the three-dimensional case,⁹ two-dimensional "pancake-shaped",²⁷ or to the "cigar-shaped" BEC's^{16,28,29} and to study the dynamics of two component BEC systems.³⁰

Acknowledgments

This work was supported in part from the Red de Macrouiversidades Públicas de America Latina Exchange Program, from the Science Division of the The City College of CUNY and from the CUNY-Caribbean Exchange Program. J. C. D-P. is grateful to UFSCar and FFCLRP-USP for hospitality. V. L-R acknowledge the financial support from Brazilian agencies FAPESP and CNPq.

APPENDIX A: VARIATIONAL CALCULATION

Inserting the wave function (5) in Eq. (1) follows the Eq. (7), where α , β , and γ are numbers equal to:

$$\gamma = \int_{-\infty}^{\infty} \sec h^4 z dz = \frac{4}{3}, \quad (\text{A1})$$

$$\alpha = 2\gamma - \int_{-\infty}^{\infty} \sec h^2 z dz = \frac{2}{3}, \quad (\text{A2})$$

$$\beta = \int_{-\infty}^{\infty} z^2 \sec h^2 z dz = \frac{\pi^2}{6} \quad (\text{A3})$$

APPENDIX B: MATRIX ELEMENTS

The fourth dimensional matrix \mathbf{T} introduced in Eq. (27) is defined as

$$T_{plmn} = \frac{1}{\pi \sqrt{2^{n+m+l+p} n! m! l! p!}} \times \int \exp(-2z^2) H_n(z) H_m(z) H_l(z) H_p(z) dz. \quad (\text{B1})$$

The matrix elements T_{plmn} have the followings properties:

i) $T_{plmn} = 0$ if $n + m + l + p = \text{odd number}$.

ii) T_{plmn} is invariant under the permutation of the quantum numbers n, m, l , and p , i.e.

$$T_{plnm} = T_{lpmn} = T_{pmln} = \dots$$

iii) For $m = 0$ we find³¹

$$T_{pln0} = \frac{2^{s-1} \Gamma(s-l) \Gamma(s-p) \Gamma(s-n)}{\pi^2 \sqrt{2^{n+l+p} l! p! n!}}, \quad (\text{B2})$$

where $\Gamma(z)$ is the gamma function and $2s = n + l + p + 1$.

iv) The following relations hold between two successive matrix elements T_{pln0} :

$$T_{pln0} = \frac{(s-l-1)(s-n-1)}{(s-p)\sqrt{p(p-1)}} T_{p-2ln0}, \quad (\text{B3})$$

or

$$T_{pln0} = \frac{(s-n-1)}{\sqrt{lp}} T_{p-1l-1n0}, \quad (\text{B4})$$

with

$$T_{0000} = \frac{1}{\sqrt{2\pi}}. \quad (\text{B5})$$

v) For the most general case we have the expression³²

$$\begin{aligned} T_{p,l,n,m} &= \frac{(-1)^{M-m-p} 2^{M-\frac{1}{2}}}{\pi \sqrt{2^{n+m+l+p} n! m! l! p!}} \times \\ &\frac{\Gamma(M-l+\frac{1}{2}) \Gamma(M-n+\frac{1}{2})}{\Gamma(M-n-l+\frac{1}{2})} \times \\ &{}_3F_2 \left(\begin{matrix} -m, & -p, & -M+n+l+\frac{1}{2}; \\ -M+l+\frac{1}{2}, & -M+n+\frac{1}{2}; \end{matrix} 1 \right), \end{aligned} \quad (\text{B6})$$

where ${}_3F_2 \left(\begin{matrix} \alpha_1, \alpha_2, \alpha_3; \\ \beta_1, \beta_2; \end{matrix} 1 \right)$ is the generalized hypergeometric series³¹ and $2M = p + l + m + n$.

vi) The matrix element T_{plnm} satisfies the recurrence relation

$$T_{plnm} = \sqrt{\frac{n+1}{m}} T_{pln+1m-1} - \sqrt{\frac{l}{m}} T_{pl-1nm-1} - \sqrt{\frac{p}{m}} T_{p-1lnm-1}. \quad (\text{B7})$$

These mathematical properties allow to evaluate the tensor \mathbf{T} in a straightforward way and in consequence to solve Eq. (28) for the eigenvalues μ and eigenvector \mathbf{C} very efficiently.

-
- ¹ M. H. Anderson, J. R. Ensher, M. R. Matthews, C. E. Wieman, E. A Cornell, *Science* **269**, 198 (1995).
- ² K. B. Davis, M. -O. Mewes, M. R. Andrews, N. J. van Druten, D. S. Durfee, D. M. Kurn, and W. Ketterle, *Phys. Rev.Lett.* **75**, 3969 (1995).
- ³ C. C. Bradley, C. A. Sackett, J. J. Tollett, and R. G. Hulet, *Phys. Rev. Lett.* **75**, 1687 (1995).
- ⁴ D. J. Han, R. H. Wynar, Ph. Courteille, and D. J. Heinzen, *Phys. Rev. A* **57**, 4114 (1998).
- ⁵ T. Esslinger, I. Bloch, and T. W. Hänsch, *Phys. Rev. A* **58**, 2664 (1998).
- ⁶ L. V. Hau, B. D. Busch, Ch. Liu, Z. Dutton, M. M. Burns, and J. A. Golovchenko, *Phys. Rev. A* **58**, 54 (1998).
- ⁷ C. C. Bradley, C. A. Sackett, J. and R. G. Hulet, *Phys. Rev.Lett.* **78**, 985 (1997).
- ⁸ E. P. Gross, *Nuovo Cimento* **20** 454 (1961); L. P. Pitaevskii, *Zh. Eksp. Teor. Fiz.* **40** 646 (1961) [1961 *Sov. Phys. JETP* 13 451].
- ⁹ F. Dalfovo, S. Giorgini, L. P. Pitaevskii, and S. Stringari, *Rev. Mod. Phys.* **71**, 463 (1999).
- ¹⁰ L. Khaykovich, F. Schreck, G. Ferrari, T. Bourdel, J. Cubizolles, L. D. Carr, Y. Castin, C. Salomon., *Science* **296**, 1290 (2002); K.E. Strecker, G. B. Partridge¹, A. G. Truscott and R. G. Hulet¹, *Nature (London)* **417**, 150.(2002).
- ¹¹ S. Burger, K. Bongs, S. Dettmer, W. Ertmer, and K. Sengstock, *Phys. Rev. Lett.* **83**, 5198 (1999).
- ¹² B. Eiermann, Th. Anker, M. Albiez, M. Taglieber, P. Treutlein, K.-P. Marzlin, and M. K. Oberthaler, *Phys. Rev. Lett.* **92**, 230401 (2004).
- ¹³ L. P. Pitaevskii, *Zh. Eksp. Teor. Fiz.* **40**, 646 (1961) [*JETP* **13**, 451, (1961)].
- ¹⁴ P. A. Ruprecht, M. Edwards, K. Burnett, and C. W. Clark, *Phys. Rev. A* **54**, 4178 (1996).

- ¹⁵ A. V. Ponomarev, J. Madroñero, A. R. Kolovsky, and A. Buchleitner. Phys. Rev. Lett. **96**, 050404 (2006).
- ¹⁶ V. M. Pérez-García, H. Michinel, and H. Herrero, Phys. Rev. A **57**, 3837 (1998).
- ¹⁷ C. Trallero-Giner, J. Drake, V. Lopez-Richard, C. Trallero-Herrero, Joseph L. Birmand, Physics Letters A **354**, 115 (2006).
- ¹⁸ M. Edwards and K. Burnett, Phys. Rev. A **51**, 1382 (1995).
- ¹⁹ G. Baym and C. J. Pethick, Phys. Rev. Lett. **76**, 6 (1996).
- ²⁰ P. M. Morse and H. Feshbach, *Methods of Theoretical Physics* (NY, McGraw-Hill, 1953).
- ²¹ S. G. Mikhlin and K. L. Prössdorf, *Approximate Methods for Solutions of Differential and Integral Equations* (American Elsevier Publ. Co., NY, 1967).
- ²² I. G. Petrovskii, *Lectures on the Theory of Integral Equations* (Graylock Press, Rochester, 1957).
- ²³ *Handbook of Mathematical Functions*, edited by M. Abramowitz and I. Stegun (Dover, NY, 1972).
- ²⁴ S. G. Mikhlin, *Variational Methods in Mathematical Physics* (Pergamon Press, 1964).
- ²⁵ Bender C M and Orszag S A 1978 *Advanced Mathematical Methods for Scientists and Engineers* (NY, Mc Graw-Hill).
- ²⁶ H. Pu and N. P. Bigelow, Phys. Rev. Lett. **80**, 1130 (1998).
- ²⁷ L. Salasnich, A. Parola, and L. Reatto, Phys. Rev. A **65**, 043614 (2002).
- ²⁸ Yu. S. Kivshar, T. J. Alexander, and S. K. Turitsyn, Phys. Lett. A **278**, 225 (2001).
- ²⁹ F. Kh. Abdullaev et al., Phys. Rev. Lett. **90**, 230402 (2003).
- ³⁰ C. J. Myatt, E. A. Burt, R. W. Ghrist, E. A. Cornell, and C. E. Wieman, Phys. Rev. Lett. **78**, 586 (1997).
- ³¹ I. S. Gradshteyn and I. M. Ryzhik, *Tables of Integrals, Series and Products* (Academic, NY, 1980).
- ³² R. D. Lord, J. London Math. Soc., **24**, 101 (1949).